Environmental Science
Processes & Impacts

# Cr(VI) Uptake and Reduction by Biogenic Iron (Oxyhydr)oxides

| | |
|---|---|
| Journal: | *Environmental Science: Processes & Impacts* |
| Manuscript ID | EM-ART-04-2018-000149.R2 |
| Article Type: | Paper |
| Date Submitted by the Author: | 08-Jun-2018 |
| Complete List of Authors: | Whitaker, Andrew; North Carolina State University, Soil Science<br>Amor, Mathilde; University of Lausanne, Institute of Earth Surface Dynamics<br>Pena, Jasquelin ; University of Lausanne, Institute of Earth Surface Dynamics<br>Duckworth, Owen; North Carolina State University, Soil Science |
| | |

**Environmental Significance.** Chromium (Cr) is a widespread contaminant in the environment, where its mobility is controlled by sorption and redox processes. However, little is known about its interactions with biogenic (oxyhydr)oxides (BIOS), which are widespread in aquatic environments and have properties that are distinct from synthetic (oxyhydr)oxides. Therefore, Cr(VI) sorption to BIOS and synthetic ferrihydrite (2LFh) were investigated using wet chemical methods and X-ray spectroscopy. Under circumneutral pH and oxic conditions, BIOS sorbed a similar quantity of Cr to 2LFh, but also a reductant due to the presence of Fe(II) and organic matter. Due to the ubiquity of BIOS in the environment, our results suggest they may have a large capacity for chemical reduction of Cr(VI) despite oxic conditions.

# Cr(VI) Uptake and Reduction by Biogenic Iron (Oxyhydr)oxides

by

Andrew H. Whitaker,[1] Jasquelin Peña,[2] Mathilde Amor,[2] and Owen W. Duckworth[1,*]

[1]*Department of Crop and Soil Sciences, North Carolina State University, Raleigh, NC 27695-7620*

[2]*Institute of Earth Surface Dynamics, Faculté des Géoscience et de l'Environnement, Université de Lausanne, Géopolis, 1015 Lausanne, Switzerland*

Submittal to
April 1, 2018
Revised
May 21, 2018
Revised
June 8, 2018

Environmental Sciences: Processes and Impacts

*To Whom Correspondence Should be Addressed
owen_duckworth@ncsu.edu
Tel. (919) 513-1577
Fax. (919) 515-7959

**Abstract.** The mobility and toxicity of chromium (Cr) in soil and water systems are largely controlled by its oxidation state and interactions with solid phases. Relative to abiotic minerals, biogenic iron (Fe) (oxyhydr)oxides (BIOS) may enhance Cr(VI) adsorption and reduction due to their poorly ordered structures, large surface areas, and incorporation of cell derived organic matter. To determine the extent and mechanisms of the reaction between Cr(VI) and BIOS, sorption isotherm and kinetic studies were conducted using two-line ferrihydrite, BIOS, and BIOS amended with 0.135 M ferrozine (an Fe(II) chelator). X-ray absorption near edge structure (XANES) spectroscopy of BIOS reacted with Cr(VI) showed approximately 50% reduction of the total sorbed Cr from Cr(VI) to Cr(III) after 14 days of exposure. Sorbed Cr(III) was best fit with an organic carboxylate complex after 1 d of reaction, but after 7 d mineral-associated Cr(III) was the predominant form. In the presence of ferrozine, Cr(VI) reduction by BIOS was inhibited, confirming a key role for Fe(II) as the Cr(VI) reductant. However, the lack of a 3:1 reaction stoichiometry between Fe(II) and Cr(III) produced suggests roles for reaction with organic matter and Cr(V) autoreduction in Cr(III) production. This study thus elucidates an unrecognized mechanism of Cr sequestration by ubiquitous natural Fe (oxyhydr)oxide deposits. Furthermore, the redox transformation of mobile Cr(VI) to less soluble Cr(III) species observed in our study implies that biogenic Fe (oxyhydr)oxides in soils and natural waters may naturally attenuate Cr(VI) concentrations through sorption and reduction processes, thus limiting its transport to downstream environments.

# Introduction

Chromium is a widespread toxicant that is released to the environment through anthropogenic activities[1-3] or geogenic processes.[4, 5] It is the third most frequently found contaminant at Superfund sites,[6] where it is derived primarily from legacy industrial, agricultural, and mining activities. However, weathering of ultramafic and serpentine rocks can also result in soil and water concentrations that may threaten surface and ground water quality.[4, 7, 8] Like many transition metals, the mobility and toxicity of Cr is highly dependent upon its oxidation state.[2, 3, 8] The trivalent form, Cr(III), which occurs naturally in rocks, is an essential mammalian trace nutrient and only toxic to plants at extremely high concentrations.[9] In contrast, the hexavalent form, Cr(VI), is a human and animal carcinogen[10] that can be toxic to plants at concentrations as low as 0.5 mg $L^{-1}$ in solution and 5 mg $kg^{-1}$ in soils.[11, 12] In the environment, Cr(VI) can be transformed to Cr(III) by common reductants, including sulfides, organic matter, and ferrous iron.[2] Once reduced, Cr(III) can precipitate from solution as low solubility solids, such as $Cr(OH)_3$ or mixed Cr(III)/Fe(III) (oxyhydr)oxides.[3, 8]

Iron(III) oxides, hydroxides, and oxyhydroxides (referred to in the paper as "(oxyhydr)oxides") can influence the fate and transport of Cr(VI) via sorption reactions that occur in soils and waters.[13] Therefore, understanding the mechanisms of interactions of Cr(VI) with Fe minerals is essential to predicting its mobility and toxicity in the environment. Although most studies on the sorption of Cr(VI) by Fe (oxyhydr)oxides have utilized synthetic minerals, the formation of Fe (oxyhydr)oxides at circumneutral redox interfaces found in soils, surface waters, and engineered systems is often driven by diverse Fe oxidizing bacteria.[14-18] These microbes compete with chemical oxidation processes at suboxic environments (ca. <50 μM $O_2$), where they can account for 20–90% of oxidation.[19] These biogenic Fe (oxyhydr)oxides (BIOS)

occur in diverse environments, including surface waters,[20-22] drains,[23, 24] wetlands,[17, 25, 26] caves,[27] groundwater,[28, 29] springs,[16, 30] and mines,[31, 32] which suggests that BIOS formation is widespread where Fe-rich anoxic waters meet oxygenated fluids.

Biogenic Fe (oxyhydr)oxides have a poorly crystalline mineral structure similar to synthetic two-line ferrihydrite (2LFh),[15, 33] making them effective sorbents.[33-36] However, relative to 2LFh, they have smaller crystal domain sizes and more negative surface charges, which can affect sorption properties.[33] For example, BIOS adsorbed As(III) and As(V), U(VI), and Sr(II), Pb(II), Cu(II), and Zn(II) with maximum sorbed concentrations that varied from equal to eight-fold higher than 2LFh.[33, 37-39] In addition to structural properties that may contribute to these differences in sorption capacity, BIOS are embedded in a biofilm matrix,[19] which has the potential to profoundly impact their reactivity. The BIOS containing biofilm contains bacteria, including Fe oxidizing and reducing organisms,[15, 40] and cell-derived organic matter (CDOM), which has been shown in other BIOS deposits to be comprised predominantly of polysaccharides with contributions from proteins and other biomolecules.[32, 41, 42] Organic matter and microbial cells may directly bind metals,[43] but may also participate in redox reactions (including cryptic reactions involving Fe[44, 45]) that may favor or inhibit contaminant mobilization. Therefore, in addition to a large sorption affinity for Cr(VI), BIOS-associated microorganisms and organic matter may mediate Cr(VI) reduction.

Despite the potential for redox transformations in BIOS, studies of their reactivity with metals and anions have focused largely on sorption processes that do not involve oxidation or reduction.[46-50] Although several studies have shown that abiotic Fe (oxyhydr)oxide minerals can effectively remove Cr(VI) from aqueous solutions,[13, 51-54] few studies have considered BIOS interactions with Cr,[55] and, to the authors' knowledge, there are no existing studies investigating

the sorption of Cr(VI) to BIOS. The present work investigates the uptake of Cr(VI) by BIOS at pH 7 under oxic conditions via sorption isotherms and kinetic sorption experiments. X-ray absorption spectroscopy was employed to elucidate changes in the Fe and Cr speciation upon the reaction of Cr(VI) with BIOS. Additional experiments were conducted in the presence of ferrozine, an Fe(II)-chelator, to assess the extent to which dynamic redox processes involving Fe(II) production could impact the fate of Cr in the BIOS.

# Materials and Methods

***Materials.*** All chemicals were reagent grade or higher purity, and provided by Acros Organics, Fisher Scientific, and Sigma-Aldrich. Solutions were prepared using ASTM Type 1 (>18.2 MΩ·cm) deionized water (DI).

***Biogenic iron (oxyhydr)oxides (BIOS).*** Biogenic Fe (oxyhydr)oxides, a term used to refer to a mixture assumed to be composed of (oxyhydr)oxides of biotic and abiotic origin, organic matter, cells, and perhaps detrital materials, were collected in April of 2017 at Rocky Branch Creek adjacent to Pullen Park (35°46'49"N 78°40'01"W; Raleigh, North Carolina), where thick, clay-like mats (**Electronic supplementary information Fig S1**) of BIOS form intermittently throughout the year.[33, 56, 57] The pH (pH = 6.2 and 6.6), dissolved oxygen (DO = 65.3 μM (2.1 mg $L^{-1}$) and 220.4 μM (7.1 mg $L^{-1}$)), and temperature (20.5 and 21.8°C) were measured within the BIOS mats and mid-stream where no Fe (oxyhydr)oxides were present, respectively; stream water chemistry is reported elsewhere.[56] Disposable polypropylene (PP) spatulas were used to collect the BIOS into 50 mL PP centrifuge tubes, which were then taken to the laboratory.

In the laboratory, the BIOS were centrifuged for 10 min at 10,000 × *g*. The supernatant was decanted, and the BIOS were pooled into one 50 mL PP centrifuge tube and raised to 40 mL with DI, which was then agitated (Vortex Genie 2, Scientific Industries) to ensure adequate mixing of the BIOS. The BIOS sample was centrifuged for a final time at 10,000 × *g* for 10 min. The supernatant was discarded, and the resulting composite sample was stored in the freezer as a wet paste at -20°C until further use. Prior to freezing, a 100 mg subsample of the BIOS composite was oven-dried for 24 hours at 100°C to determine the moisture content so that a wet sample stock suspension could be used in experiments on a dry mass basis.

***Synthetic two-line ferrihydrite.*** The Schwertmann and Cornell method[58] was used to synthesize 2LFh in the laboratory. Briefly, 40 g of $Fe(NO)_3 \cdot 9H_2O$ was dissolved in 500 mL of DI under vigorous mixing on a stir plate. Upon complete dissolution, the pH of the solution was adjusted to 7.5 ± 0.5 with 330 mL of 1 M KOH, with the last 20 mL added in a dropwise fashion. The pH was held constant at 7.5 ± 0.5 for 30 minutes before transferring into six 50 mL PP centrifuge tubes. The suspensions were then centrifuged at 10,000 × *g* for 10 min, the supernatant was decanted, and the remaining solids were rinsed with DI. This centrifuge-rinse cycle was repeated four more times. The suspensions were combined into one 50 mL PP centrifuge tube and centrifuged a final time at 10,000 × *g* for 10 min, and the supernatant was discarded. A 100 mg aliquot of the wet paste was oven-dried for 24 h at 100°C to determine moisture content in order to accurately apply wet solid loadings based off of a dry mass basis. The final product yielded approximately 10 g of 2LFh on a dry mass basis, which was stored in the freezer at -20°C until further analyses.

***Sorbent characterization.*** The BIOS and 2LFh were analyzed for elemental composition. The C and N content of the BIOS was determined by total combustion using a Perkin Elmer Series II-2400 CHNS/O analyzer. For metal, P and S analyses, approximately 50 mg of dry solids were dissolved with 10 mL each of concentrated trace metal HCl and $HNO_3$ acid, and then diluted to 40 mL with DI. The digestions were shaken by hand and then incubated at room temperature for one hour before filtration through 0.22 µm nylon filters (VWR International). The BIOS filtrates were then analyzed for Fe, Mn, Al, Ca, Si, K, Mg, Na, Cr, Cu, Pb, Zn, S, and P by using a Perkin Elmer Optima 8000 ICP-OES spectrometer, whereas the 2LFh filtrate was only analyzed for Fe. An HCl acid digestion was used to extract any Fe(II) stabilized within the BIOS. Samples (20 mg) of dry solids were allowed to dissolve in 10 mL of concentrated HCl acid for one hour before filtering with a 0.22 µm nylon filter (VWR International). The filtrate was diluted to 40 mL with DI and analyzed for Fe(II) using a VWR V-1200 series UV-visible spectrophotometer according to a modified version of the Stookey method.[59] Briefly, 1 mL of 0.01 M ferrozine and 2 mL of DI, were added to 1 mL of sample. The sample was buffered to pH = 7.5 ± 0.1 using 1 mL of 5 M ammonium acetate leading to a final ferrozine concentration of 0.002 M.

The 2LFh and BIOS were also characterized according to mineral phase and specific surface areas. For X-ray diffraction (XRD) analysis, 200 mg of air dried BIOS and 2LFh were loaded onto a glass sample holder and analyzed with a Rigaku SmartLab X-ray diffractometer with graphite monochromated Cu K-α radiation. The samples were scanned from 10–80° 2θ in 0.05° increments. Iron K-edge X-ray absorption spectroscopy (XAS) was also used to characterize the minerals in terms of short-range structure (< 6 Å), as described below. Finally, $N_2$ (g) adsorption Brunauer-Emmett-Teller (BET) specific surface area was determined with a Quantachrome Monosorb (MS-17).

***Kinetics of Cr(VI) sorption by BIOS and 2LFh.*** All sorption kinetic studies were performed in duplicate by adding BIOS and 2LFh stock suspensions to 50 mL PP centrifuge tubes to achieve a sorbent concentration of 1 g solid $L^{-1}$ on a dry weight basis, which is equivalent to 0.13 and 0.20 mM Fe, respectively. A 19.23 mM Cr stock solution was made via the addition of $Na_2CrO_4$ into a 1L volumetric flask and raised to volume with 0.01 M NaCl. The pH of the stock solution was adjusted to pH = 7.0 ± 0.1 using 1 M HCl. Four different treatments were chosen to investigate Cr sorption by BIOS as well as any differences in Cr interactions with BIOS relative to 2LFh: 1) control (no sorbent) with 0.96 mM Cr (50 mg Cr $L^{-1}$); 2) 2LFh with 0.96 mM Cr; 3) BIOS with 0.96 mM Cr; and 4) BIOS with 0.96 mM Cr and 0.135 M ferrozine, an Fe(II) chelator (log$K$ = 15.56)[60] used to complex Fe(II).[59, 61-63] The Cr concentration is similar to those found in contaminated groundwater (0.04–5.77 mM),[45, 64-67] and facilitates comparison with previous experiments[12, 52, 53, 68-71] and collection of X-ray absorption spectra. All sorbent suspensions were adjusted to pH = 7.0 ± 0.1 using 1 M NaOH in 0.01 M NaCl to mimic the circumneutral stream water associated with BIOS formation.

Experiments were started by placing samples on an end-over-end sample rotator (Scilogex MX-RD-Pro) at 25 rpm. Suspension pH was maintained at pH = 7.0–7.2 by addition of small quantities of 0.1 M HCl, with drift between adjustments being less than 0.3 units; pH was stable after 24 h. At each sampling time point (1, 3, 7, and 14 d), dissolved oxygen concentrations were measured by using an Ocean Optics Neofox oxygen probe. Subsequently, individual tubes were removed from the rotator and centrifuged at 10,000 × $g$ for 10 min. The supernatant was filtered by syringe using a 0.22 μm nylon filter (VWR International) into 50 mL

PP centrifuge tubes. The adsorbent and filtrate were stored in the freezer at -20°C until further analyses.

Each filtrate was subdivided into three aliquots. The first was diluted with 1% $HNO_3$ and analyzed for total $Fe_T$ and $Cr_T$ with a Thermo Scientific iCE 3000 Atomic Absorption Spectrometer (AAS). Analytical quality assurance was monitored by analyzing a 1% $HNO_3$ blank every tenth sample and by running a mid-range calibration standard at the end of every analysis. The second was analyzed for Fe(II) concentrations using a modified version of the Stookey method,[59] as described above. The treatment that already had ferrozine was buffered with 1 mL of ammonium acetate and diluted to a final ferrozine concentration of 0.002 M with deionized water. Samples were analyzed in duplicate at $\lambda$ = 562 nm and compared to a standard curve that ranged from 0–72 μM Fe(II). The final aliquot was used for Cr(VI) quantitation by colorimetry.[72] Briefly, 1 mL of each sample was diluted to 8 mL using deionized water. One milliliter of a 3.1 mM s-diphenylcarbazide stock was then added to the diluted sample and incubated for 20 min to facilitate color development. Samples were analyzed in duplicate at 540 nm and compared to a standard curve that ranged from 0–38 μM Cr(VI). The measured Cr(VI) concentrations were within 7% of $Cr_T$ measured by AAS, which is within the combined error ($\sqrt{\sum Error_{CrT}^2 + Error_{Cr(VI)}^2}$) of the AAS and photometric methods, indicating that, with in uncertainty, dissolved $Cr_T$ is equivalent to Cr(VI). Thus, all data are reported in terms of $Cr_T$ for simplicity.

***Adsorption isotherms.*** Chromium adsorption isotherms were conducted with the 2LFh and BIOS sorbents according to similar procedures to those of Sowers et al.[33] Experiments were initiated by adding a known amount of the wet BIOS and 2LFh in order to achieve a 1 g $L^{-1}$ sorbent on a

dry mass basis (0.13 and 0.20 mM Fe, respectively). Sodium chromate ($Na_2Cr(VI)O_4$) was used to make a 9.62 mM (500 mg $L^{-1}$ Cr(VI)) stock solution in 0.01 M NaCl at pH = 7.0 ± 0.1. An aliquot of the Cr(VI) stock solution was pipetted into 50 mL PP centrifuge tubes in order to achieve Cr(VI) concentrations ranging from 0–1.92 mM, which are similar concentrations to those used in previous experiments.[53] The pH was adjusted to pH = 7.0 ± 0.1 using 0.1 M HCl or 0.1 M NaOH, and samples were diluted to final volume (20 mL) with 0.01 M NaCl. The samples were then placed onto a tube rotator at 25 rpm. The pH of the adsorption experiments was monitored at t = 0, 3, 24, and 48 h and, if needed, adjusted with 0.1 M NaOH or 0.1 M HCl in order to maintain pH = 7.0 ± 0.1. At t = 48 h (attainment of pseudo-equilibrium),[73-75] the experiments were centrifuged at 10,000 × *g* for 10 min, followed by filtration of the supernatant with a 0.22 µm nylon filter (VWR International). The filtrate was then stored at 4°C until further analysis. All adsorption isotherms were performed in duplicate.

Aqueous $Cr_T$ concentrations were measured by using AAS. The sorbed concentration of Cr was determined from the difference in concentration before and after the sorption reaction. Non-linear optimization was performed in a preprogrammed Excel spreadsheet[76] and used to fit the Cr isotherm data with a Freundlich isotherm model, which provided better fits than a Langmuir model in all cases (as judged by model goodness of fit parameters). The uncertainty on Freundlich model parameters is reported as standard error.

***X-ray absorption spectroscopy.*** Iron and Cr K-edge X-ray absorption spectra (XAS) were collected in July of 2017 at beamline 11-2 at the Stanford Synchrotron Radiation Lightsource (SSRL). All BIOS and 2LFh samples were loaded onto aluminum sample holders as wet pastes and kept moist by sealing with kapton tape. All Fe K-edge spectra were collected at room

temperature in fluorescence mode with a Lytle detector. Cr K-edge spectra were collected in a liquid nitrogen (LN2) cryostat in fluorescence mode using a 100-element Ge detector. Monochromator energy was calibrated by adjusting the first derivative maxima of the Fe and Cr foils to the element binding energies of 7112 and 5989 eV, respectively. The incident beam was energy selected using a Si (220) double-crystal monochromator, and harmonics were rejected with a cut-off rhodium coated mirror at an energy of 10,500 eV. Iron and Cr fluorescence spectra were collected using Soller slits and a Z-1 X-ray filter (Mn and V, respectively). For selected Fe and Cr samples, multiple spectra were collected for each sample, with no evidence of beam damage in successive scans, and averaged to improve the signal-to-noise ratio.

Spectra were energy calibrated, averaged, background-subtracted, splined as described by Kelly et al.[77] using the SIXPACK interface,[78] which is built on the IFEFFIT code.[79] To determine oxidation state, Fe K-edge XANES spectra were analyzed by linear combination fitting (LCFs) from 7100–7200 eV using ferrihydrite and pyrite standards, which are used as Fe(III) and Fe(II) standards, respectively. The reported fits are normalized to 100%, with the raw summation ranging from 99–100 ± 1%. For Cr K-edge XANES spectra, the area of the pre-edge feature was used to quantify the oxidation state (i.e., the percentage of Cr(VI) and Cr(III)) of Cr sorbed to Fe (oxyhydr)oxides.[77, 80] The area of the Cr pre-edge peak located at 5993.3 eV, which is diagnostic of Cr(VI), was integrated using KaleidaGraph Version 4.5 (Synergy Software, Reading, PA, USA). The integrated areas of the Cr pre-edge peaks were compared to a calibration curve based on spectra of known mixtures of $Cr(III)_2O_3$ and $K_2CrO_4$ following established procedures, [77 80] yielding a fraction of Cr(VI) with an estimated uncertainty of 10%.[77 80]

Additional LCF analysis was conducted to estimate the chemical speciation of Fe and Cr. Iron K-edge extended X-ray absorption fine structure (EXAFS) spectra were fit with a set of mineral standards[81-83] listed in **Table S1**, with those used for the final fits listed in bold italic. For Cr K-edge XANES, spectra were fit from 5980–6080 eV with Cr(VI) sorbed to 2LFh (14 day sample, with oxidation state confirmed to be ~100% Cr(VI) by the analysis above), as well a published organic Cr(III)-siderophore complexes (e.g., Cr(III)-rhizoferrin)[84] and a mixed Cr(III)/Fe(III)$OH_3$ mineral standard (Cr2Fe8 from Saad et al.[85]). Standards that made up less than 10% of LCFs were removed, and fits were recalculated using the remaining standards. The reported fits are normalized to 100%, with the raw summation ranging from 70–109 ± 2–8% for Fe K-edge EXAFS and 100-107 ± 4% for Cr K-edge XANES. The uncertainty reported for LCFs is the software output; however, this is known to be an underestimate, and uncertainty is assumed to be approximately 10%.[86, 87]

# Results and Discussion

***Sorbent composition, structure, and specific surface area.*** The elemental composition of BIOS and 2LFh are presented in **Table S2.** The BIOS consists primarily of Fe, Si, and C with concentrations of 370.4, 11.9, and 68.5 g $kg^{-1}$ solid (dry basis), respectively. These major element concentrations are within the range reported for natural Fe (oxyhydr)oxides.[14, 33, 55, 88, 89] The BIOS contained smaller proportions (≤ 6.0 g $kg^{-1}$ solid) of Al, Mn, Ca, K, Mg, Na, Cr, Pb, Zn, Cu, P, S, and N, which is consistent with those reported for natural Fe (oxyhydr)oxides sampled from a California mercury mine[88] and the Juan de Fuca Ridge in the Pacific Ocean.[89] Native Cr concentrations within the BIOS were below 0.2 μM Cr (< 0.02 g Cr $kg^{-1}$ solid). Less than 0.2% (1.8 g Fe(II) $kg^{-1}$ solid; this translates to 33 μM if dissolved) of the total Fe in the

initial sorbent was found to be Fe(II), as measured by acid extraction followed by the ferrozine assay. Although the initial Fe(II) concentration within the BIOS may be overestimated due to the potential for enhanced reduction of Fe(III) to Fe(II) by organic matter at low pH,[1] Lovely and Phillips have shown that HCl acid digests of Fe(II) and organic matter rich sediments spiked with amorphous Fe (oxyhydr)oxides showed no increase in Fe(II) concentrations.[90] This low Fe(II) concentration is consistent with LCFs of XANES spectra **(Figure S2)**, which are best fit by 100% ferrihydrite and thus indicate the absence of detectable Fe(II) (<10%) in the samples. Synthetic 2LFh contained 553.3 g Fe $kg^{-1}$ solid, consistent with its reported composition.[33, 91]

X-ray diffraction data for 2LFh and the BIOS are presented in **Figure S3**. Synthetic 2LFh has two broad diffraction peaks at approximately 35 and 62 °2Θ, which correspond to d-spacings of 2.55 Å and 1.5 Å, respectively. Like 2LFh, the BIOS has two broad diffraction maxima; however, there are noticeable differences. First, the BIOS diffraction peaks are considerably broader than 2LFh which has been reported for natural Fe (oxyhydr)oxides and 2LFh samples containing Al, Si, and organic C.[88, 92-94] Second, slight shifts in peak positions towards lower °2Θ can be seen in the BIOS, which are consistent with the effect of Si and organic C incorporation on the diffraction pattern of 2LFh.[92, 94] These peak shifts suggest that there is an subtle increase in structural strain or decrease in particle size of the BIOS when compared to 2LFh[88], and confirms intimate association of CDOM and mineral.

Iron K-edge EXAFS spectra of the unreacted BIOS (Day 0) and 2LFh are plotted along with Fe(III) mineral standards for comparison in **Figure 1**; LCFs are shown as black dotted lines with fit parameters in **Table 1**. The 2LFh EXAFS spectrum was best fit with a XAS ferrihydrite standard;[95] the BIOS spectrum was best fit with the ferrihydrite standard and hydrous ferric (oxyhydr)oxide with silica standard at 80 ± 4% and 20 ± 2% contributions, respectively. When

comparing visually the Fe K-edge EXAFS spectra from the BIOS to 2LFh, the EXAFS spectrum shows a dampened beat pattern at $k$ = 7–8 Å$^{-1}$ for BIOS, which is consistent with a decrease in corner-sharing Fe-O octahedra.[96, 97] Thus, EXAFS results indicate that the BIOS has a less ordered structure than 2LFh, consistent with our XRD data and other observations of natural Fe (oxyhydr)oxides.[33, 88, 97, 98] Finally, BET specific surface area (SSA) of the BIOS and 2LFh were determined to be 143 and 266 m$^2$ g$^{-1}$, respectively, which agrees well with the ranges of SSAs reported for other natural Fe (oxyhydr)oxides collected from similar environments (65–312 m$^2$ g$^{-1}$; mean = 168 m$^2$ g$^{-1}$, $n$ = 9 ).[33, 88, 99]

***Sorption of Cr to 2LFh and BIOS.*** Previous work has suggested that BET surface area is the most effective way to normalize for variation in the sorption properties of different BIOS samples.[33] The BET SSA normalized sorption of Cr to 2LFh and BIOS as a function of time is shown in **Figure 2A**. Both sorbents show a gradual increase in Cr sorption from day 1 through day 14 that ranges from approximately 0.9 to 1.3–1.7 μmol Cr m$^{-2}$. The presence of ferrozine did not have a large impact on extent of Cr sorption to BIOS, which reached a maximum of 1.48 μmol m$^{-2}$ at 14 d.

**Figure 3** shows the BET SSA normalized sorption of Cr onto synthetic 2LFh and BIOS as a function of dissolved Cr concentration after 48 h of equilibration. For both 2LFh and BIOS, the Cr surface concentration increases with increasing dissolved Cr concentrations. The slope of the curves decreases with increasing dissolved Cr concentrations, which is typical for L-type isotherms.[100] When normalized to sorbent mass (**Figure S4**) both sorbents show similar sorption behavior. For example, at dissolved concentrations around 1000 μM Cr, synthetic 2LFh and BIOS sorbed 255 and 235 μmol Cr g$^{-1}$, respectively. These values are larger than the reported

162 and 93 μmol Cr $g^{-1}$ for poorly-crystalline $Fe(OH)_3$ and akageneite at pH = 7 and similar dissolved Cr concentrations.[53] These discrepancies in Cr sorption may arise due to differences in sorbent preparation (oven dried at 50°C vs wet paste), sorbate to sorbent contact time (3 vs 48 h), solids loadings, and specific surface area.[34]

Sorption for BIOS and 2LFh data were modeled with a Freundlich isotherm.[76] The Freundlich sorption constant ($K_f$) and exponential constant ($n$) for synthetic 2LFh was 0.009 ± 0.005 μmol Cr $m^{-2}$ and 0.69 ± 0.07, respectively, whereas, for BIOS they were 0.020 ± 0.006 μmol Cr $m^{-2}$ and 0.63 ± 0.04, respectively. The 2-fold larger $K_f$ for BIOS may be due to the poorer ordering of the BIOS[33, 88, 97, 98] (**Figure 1 and Table 1**), as evidenced in our XRD and XAS measurements, and has been observed for natural Fe (oxyhydr)oxides when compared to synthetic 2LFh.[88] Previously reported $K_f$ values for As(III) and As(V) were 1.2–2.5 times higher for BIOS than for 2LFh.[33]

***Reduction of Cr(VI) by BIOS.*** The pre-edge features of Cr K-edge XANES spectra were used to determine the proportion of Cr(III) and Cr(VI) sorbed to Fe (oxyhydr)oxides. The mole % of Cr(VI) and Cr(III) sorbed to synthetic 2LFh and BIOS are summarized in **Figure 4 A-C** and **Table S4**.[77, 80] For all sampling times, the pre-edge feature in the XANES spectra of Cr sorbed to synthetic 2LFh (**Figure 4A**) is similar in size to the $K_2CrO_4$ reference spectrum, suggesting Cr bound to 2LFh is predominantly Cr(VI) with little variation over time. When quantified by comparison of integrated peak area to known standards, Cr(VI) accounted for ≥90 ± 9% of the total Cr sorbed to 2LFh at all sampling times (**Figure 4D**). In contrast, BIOS samples show a clear decrease in the pre-edge intensity and area with increasing reaction time; by day 14, the XANES pre-edge feature resembles the 50% Cr(VI) standard (**Figure 4B**), thus indicating

substantial reduction of Cr(VI) to Cr(III). Fits to the pre-edge feature show that, the percentage of Cr(VI) sorbed to BIOS decreased quickly during the first day and then gradually from 73 ± 7% to 55 ± 6% from day 2 to day 14. In addition to reduction in pre-edge intensity, the BIOS spectra also show changes in the shape of the edge and post-edge regions of the XANES spectra as a function of time.

The BIOS samples with the 0.135 M ferrozine treatment showed XANES spectra (**Figure 4C**) that resemble that of the Cr(VI) standard for all sampling days. When quantified by pre-edge peak area, sorbed Cr in the BIOS with 0.135 M ferrozine treatment at day 1 and 14 was 93 ± 9% Cr(VI) and 95 ± 9 % Cr(VI), respectively, with minor variations at day 3 and 7. These results thus indicate that ferrozine inhibited Cr(VI) reduction. Similarly, Buerge and Hug[1] showed that the reduction of Cr(VI) by Fe(II) was inhibited in the presence of 1,10-phenanthroline, a related Fe(II) chelator. Furthermore, control experiments containing ferrozine (0.135 M) and Cr(VI) (0.96 mM), showed no Cr(VI) reduction to Cr(III), as determined by no loss of Cr(VI) from solution over 7 days (data not shown).

Careful inspection of the white line of the Cr K-edge XANES spectra reveals systematic changes to the BIOS spectra as a function of time. In addition to the reduction in size of the pre-edge peak, a subtle increase in white line height at 6010 eV, as well as an increase in amplitude at 6023 eV, can be seen as reaction time increases from 1d to 14 d (**Figure 5A**). These changes motivated an LCF analysis that was performed on BIOS samples to determine the Cr(III) speciation (**Table S3**). For the day 1 sample, the LCF (**Figure 5A**) contained sorbed Cr(VI) and an organic Cr(III)-carboxylate complex[84] (i.e., Cr(III)-rhizoferrin (15%) and sorbed Cr(VI) (85%)). The percentage of sorbed Cr(VI) trends downward in samples collected from day 3 to day 14 (reaching 52%). By day 7, the Cr(III)-rhizoferrin component decreased to <10% in LCFs.

In contrast, the mineral associated Cr(III) component (Cr2Fe8,[85] a 20% solid Cr-Fe (oxyhydr)oxide solid solution) increased from <10% at day 1 to 48% in day 14. Proportions of Cr(VI) determined by LCFs are slightly lower with those derived from the pre-edge peak calibration method for samples collected on days 1 and 3 but were within fitting uncertainty of each other on days 7 and 14, indicating reasonable agreement between the methods (**Table S4**). This analysis indicates that Cr(VI) reduced to Cr(III) by BIOS is initially bound by the CDOM associated with the assemblage; however, as the reaction time progresses, mineral-associated Cr(III) predominates. Similarly, Wang et al.[101] showed that Cu(II) and Pb(II) increasingly partitioned to mineral surfaces ($\alpha$-$Al_2O_3$ and $\alpha$-$Fe_2O_3$) at longer exposure times (20–24 hours) compared with shorter exposure times (≤ 3 hours) in CDOM associated mineral samples.

***Fe(II) Production by BIOS.*** Total dissolved Fe concentrations for all treatments and Fe(II) production for the BIOS treatment with 0.135 M ferrozine as a function of time are presented in **Figure 2B**. Total dissolved Fe concentrations for synthetic 2LFh and BIOS remained constant at ≤ 3 μM Fe at all sampling times, which may be the result of colloidal or complexed Fe(III).[14] Aqueous Fe(II) concentrations were at or below detection limit [≤ 1.8 μM Fe(II)] in the absence of ferrozine. However, dissolved Fe concentrations for the BIOS with 0.135 M ferrozine treatment increased monotonically from 22 μM at day 1 to 90 μM at day 14. We infer that the same processes that lead to Fe(II) production from BIOS in the presence of ferrozine also lead to Fe(II) production, albeit undetectably, in the absence of ferrozine. The effective scavenging potential of Cr(VI) for Fe(II) and large dissolved oxygen concentrations (> 230 μM $O_2$) may give rise to the undetectable Fe(II) concentration seen in the BIOS treatment, even with continuous Fe(II) production.

Previous research has shown that Fe(II) produced by redox cycles of Fe (oxyhydr)oxides may reduce Cr(VI)[87]. The initial pulse in dissolved Fe(II) concentrations at day 1 is consistent with the release of the 33 μM Fe(II) initially present within the BIOS, as determined by acid extraction of the BIOS at day zero. From day 1 to 14, the amount of Fe(II) produced in the presence of ferrozine was approximately three-fold larger than the initial concentration of Fe(II) in the BIOS, with Fe(II) produced at an average rate of ~ 5 μM $day^{-1}$. The LCFs of the Fe K-edge XANES and EXAFS spectra for 2LFh and all BIOS treatments post-Cr sorption (day 14) show no significant difference relative to pre-sorption samples (**Figure 1** and **Table 1, Figure S2)**, indicating no detectable changes to the BIOS structure or oxidation state. In contrast to experiment with BIOS and ferrozine, experiments with 2LFh in the presence of ferrozine revealed no production of Fe(II) (data not shown).

The production of Fe(II) in the BIOS occurred despite dissolved oxygen concentrations (data not shown) of > 230 μM $O_2$ (7.4 mg $L^{-1}$) in all samples. Thus, the bulk solution within the suspension remains oxic, although suboxic or anoxic microenvironments may form within biomineral aggregates. Under aerobic conditions, Fe(II) is subject to rapid reoxidation[102, 103] unless stabilized by a high affinity ligand, such as ferrozine ($\log K$ = 15.56)[60]. Thus, in the absence of ferrozine, BIOS produces Fe(II) as an intermediate that may react with Cr(VI) or dissolved $O_2$ to reoxidize to Fe(III). The nature of the BIOS, which is comprised of intimate mixtures of Fe (oxyhydr)oxides, CDOM,[32, 41, 42] and microorganisms (including Fe-reducing bacteria), provides multiple pathways for Fe(II) production.[15, 40] For instance, either biological dissimilatory Fe reduction[104] or direct chemical reduction of Fe(III),[105] possibly in anaerobic microsites that can form in bio-mineral assemblages[106] may contribute to Cr(VI) reduction.

Although identifying the mechanism of Fe(III) reduction in BIOS is beyond the scope of this study, additional work is underway to determine the underlying mechanism.[107]

***Mechanisms of Cr(VI) reduction by BIOS.*** Our data show that Cr(VI) is reduced upon reaction with BIOS but not 2LFh. In addition, the presence of ferrozine, a high affinity Fe(II) chelator that was used as a trapping agent to scavenge Fe(II),[59, 61-63] inhibits the reduction of Cr(VI), indicating that Fe(II) is necessary for reduction. Previous studies have shown that Fe(II) can reduce Cr(VI) according to:

$$\mathrm{Cr(VI)} + 3\mathrm{Fe(II)} \leftrightarrow \mathrm{Cr(III)} + 3\mathrm{Fe(III)} \quad (1)$$

where Fe(II) represents a solid or aqueous species, with the reaction rate varying with the speciation of Fe(II) and Cr(VI).[1, 3, 108] In the absence of complexing agents, the rate of Fe(II) reduction of Cr(VI) is >1000-fold larger than the rate of Cr(VI) reduction by $O_2$ at circumneutral pH,[108] suggesting Fe(II) produced by BIOS will react preferentially with Cr(VI), even in fully oxygenated systems.

For Fe(II) to be the only Cr(VI) reductant in the current experiments, the stoichiometry (3:1) in equation 1 would require the production of 230 μM Fe(II). However, after 14 days of reaction, the dissolved Fe concentration produced by the BIOS with the ferrozine treatment was 90 μM (**Figure 2B**). In **Figure 6**, Cr(III) produced by BIOS (as derived from LCF fits) is plotted against Fe(II) trapped by ferrozine in BIOS experiments containing ferrozine at the corresponding time. Although this line is based only on a few points, a regression line ($R^2$ = 0.82) has a slope of near unity and an intercept near zero, which are consistent with a 1:1 reaction between Cr(VI) and Fe(II). It is possible Fe(II) may be produced and not trapped by ferrozine,[109] but we did not observe reduction of Cr(VI) to Cr(III) in our XANES results with

BIOS in the presence of ferrozine. Thus, our results suggest that no additional reactive Fe(II) was produced in the samples beyond the Fe(II) trapped by ferrozine.

Based on this analysis and our finding that Cr(III) was initially present as a Cr(III)-organic species and later as a Cr(III)-inorganic species, we can propose a mechanism for the reduction of Cr(VI) by BIOS (**Figure 7**). Fe(II) is required for Cr(VI) reduction in our system, but direct reduction of Cr(VI) by Fe(II) alone cannot explain the measured extent of Cr(III) production.[1] We thus construct a reaction scheme in which Fe(II) initiates the reduction of Cr(VI) to Cr(V):

$$\text{Cr(VI)} + \text{Fe(II)} \leftrightarrow \text{Cr(V)} + \text{Fe(III)} \quad (2)$$

Reaction 2 is consistent with the similar total Fe(II) and Cr(III) concentrations produced in the BIOS samples (90 and 77 μM, respectively) and the apparent (1:1) stoichiometry established in **Figure 6**. Previous studies have shown that the rate limiting step for reduction is the one-electron reduction of Cr(VI) to a Cr(V) intermediate;[108] in fact, Cr(V) may self-reduce to Cr(III) (with concomitant production of $O_2$) in the absence of other reductants:[110]

$$\text{Cr(V)} \leftrightarrow \text{Cr(III)} + O_2 \quad (3)$$

This reaction may contribute to our observed stoichiometry.

However, we note that CDOM is abundant in our system and can also be reactive with Cr(V) intermediates, and thus propose an alternate reaction pathway. The production of Cr(V) may facilitate reaction with abundant organic matter associated with the BIOS:

$$\text{Cr(IV,V)} + \text{CDOM} \leftrightarrow \text{(oxidized CDOM)-Cr(III) complexes} \quad (4)$$

The subsequent reduction of Cr(V) to Cr(III) is fast,[1] implying the Cr species in reaction 4 may be highly reactive. This pathway is supported by our Cr K-edge XANES LCFs, which show that Cr(III) is initially bound to a carboxylate complex within the BIOS (**Figure 5**). The formation of

these complexes implies that Cr(III) is produced near organic complexing agents, further supporting reaction 3. However, from our data it is not possible to distinguish between or determine the relative importance of contributions from reactions 3 and 4, nor the relative contribution of bacterial cells or biotic processes to the overall mechanism depicted in **Figure 7**.

***Conclusions and Environmental Implications.*** Our data suggests that, under oxic conditions, BIOS sorb Cr(VI) to a similar extent as to 2LFh, but BIOS also can reduce a fraction of the sorbed Cr(VI) to Cr(III). In general, Cr(III) is considered to be a less mobile and toxic form of Cr.[2, 3, 8] Furthermore, LCFs of Cr K-edge XANES spectra indicate that Cr(III) at longer reaction times (> 7 d) is predominantly associated with Fe minerals (BIOS). Mixed Cr(III)-Fe(III) (oxyhydr)oxides are sparingly soluble species under oxic conditions at circumneutral pH[3, 8] that are often the product of Cr(VI) reduction in the presence of Fe(II),[111] and may represent an effective sink for Cr(VI). Because BIOS are common in aquatic and soil environments,[16, 17, 97, 98, 112, 113] our results suggest that they may attenuate aqueous Cr concentrations in diverse ecosystems. Additionally, our proposed mechanism (**Figure 7**), which has a lower than 3:1 Fe(II): Cr(VI) stoichiometry (cf. reaction 1 and 2), suggests that a small concentration of Fe(II) in soils or water may drive reduction of Cr(VI). In many cases, Fe-rich soils can rapidly produce Fe(II) or harbor stable Fe(II) even in aerobic environments.[114] This suggests these environments may be able to facilitate chemical reduction of Cr(VI) regardless of aerobic status.

**Acknowledgements.** We are grateful for support received from the National Science Foundation Geobiology and Low-Temperature Geochemistry Program (award EAR-1255158). This work was supported by the U.S. Department of Agriculture National Institute of Food and Agriculture,

Hatch project NC02440. JP acknowledges support from the Sandoz Foundation and the BCV Foundation. We thank Benjamin Uster, Ching-Chang Chung, Kim Hutchison, Lisa Lentz, Guillermo Ramirez, Will Messinger, Emma Rieb, and Ryan Davis for their assistance on this project. We thank Dean Hesterberg, Yuanzhi Tang, and Nelson Rivera for reference XAS spectra. This work was performed in part at the Analytical Instrumentation Facility (AIF) at North Carolina State University, which is supported by the State of North Carolina and the National Science Foundation (award number ECCS-1542015). The AIF is a member of the North Carolina Research Triangle Nanotechnology Network (RTNN), a site in the National Nanotechnology Coordinated Infrastructure (NNCI). This work was performed in part at the Environmental and Agricultural Testing Service laboratory (EATS), Department of Crop and Soil Sciences, at North Carolina State University. Use of the Stanford Synchrotron Radiation Lightsource, SLAC National Accelerator Laboratory, is supported by the U.S. Department of Energy, Office of Science, and Office of Basic Energy Sciences under Contract No. DE-AC02-76SF00515.

## References


1. I. J. Buerge and S. J. Hug, Influence of organic ligands on chromium (VI) reduction by iron (II), *Environmental science & technology*, 1998, **32**, 2092-2099.
2. S. E. Fendorf, Surface reactions of chromium in soils and waters, *Geoderma*, 1995, **67**, 55-71.
3. F. C. Richard and A. C. Bourg, Aqueous geochemistry of chromium: a review, *Water Research*, 1991, **25**, 807-816.
4. C. Oze, D. K. Bird and S. Fendorf, Genesis of hexavalent chromium from natural sources in soil and groundwater, *Proceedings of the National Academy of Sciences*, 2007, **104**, 6544-6549.
5. A. Vengosh, R. Coyte, J. Karr, J. S. Harkness, A. J. Kondash, L. S. Ruhl, R. B. Merola and G. S. Dywer, Origin of hexavalent chromium in drinking water wells from the piedmont aquifers of North Carolina, *Environmental Science & Technology Letters*, 2016, **3**, 409-414.
6. D. Duonghong, J. Ramsden and M. Grätzel, DYNAMICS OF INTERFACIAL ELECTRON-TRANSFER PROCESSES IN COLLOIDAL SEMICONDUCTOR SYSTEMS, *J. Am. Chem. Soc.*, 1982, **104**, 2977.
7. D. M. Hausladen and S. Fendorf, Hexavalent Chromium Generation within Naturally Structured Soils and Sediments, *Environmental science & technology*, 2017, **51**, 2058-2067.
8. D. Rai, L. Eary and J. Zachara, Environmental chemistry of chromium, *Science of the Total Environment*, 1989, **86**, 15-23.
9. R. J. Bartlett and B. James, Mobility and bioavailability of chromium in soils, *Chromium in the natural and human environments*, 1988, **20**, 571.
10. D. Duonghong, E. Borgarello and M. Grätzel, Dynamics of light-induced water cleavage in colloidal systems, *J. Am. Chem. Soc.*, 1981, **103**, 4685.
11. I. J. Buerge and S. J. Hug, Influence of mineral surfaces on chromium (VI) reduction by iron (II), *Environmental Science & Technology*, 1999, **33**, 4285-4291.
12. S. E. Fendorf and G. Li, Kinetics of Chromate Reduction by Ferrous Iron, *Environmental Science & Technology*, 1996, **30**, 1614-1617.
13. P. R. Grossl, M. Eick, D. L. Sparks, S. Goldberg and C. C. Ainsworth, Arsenate and chromate retention mechanisms on goethite. 2. Kinetic evaluation using a pressure-jump relaxation technique, *Environmental Science & Technology*, 1997, **31**, 321-326.
14. O. W. Duckworth, S. J. Holmström, J. Peña and G. Sposito, Biogeochemistry of iron oxidation in a circumneutral freshwater habitat, *Chemical Geology*, 2009, **260**, 149-158.
15. D. Emerson, E. J. Fleming and J. M. McBeth, Iron-oxidizing bacteria: an environmental and genomic perspective, *Annual review of microbiology*, 2010, **64**, 561-583.
16. D. Emerson and N. P. Revsbech, Investigation of an iron-oxidizing microbial mat community located near Aarhus, Denmark- Field studies, *Appl. Environ. Microbiol.*, 1994, **60**, 4022-4031.
17. D. Emerson and J. V. Weiss, Bacterial iron oxidation in circumneutral freshwater habitats: findings from the field and the laboratory, *Geomicrobiology Journal*, 2004, **21**, 405-414.
18. F. G. Ferris, Biogeochemical properties of bacteriogenic iron oxides, *Geomicrobiol. J.*, 2005, **22**, 79-85.

19. H.-C. Flemming and J. Wingender, The biofilm matrix, *Nature Reviews Microbiology*, 2010, **8**, 623-633.
20. J. G. Jones, Some observations on occurrence of iron bacterium *Leptothrix ochracea* in fresh-water, including reference to large experimental enclosures, *J. Appl. Bacteriol.*, 1975, **39**, 63-72.
21. S. P. Sheldon and D. K. Skelly, Differential colonization and growth of algae and ferromanganese-depositing bacteria in a mountain stream, *J. Freshwat. Ecol.* , 1990, **5**, 475-485.
22. H. Lünsdorf, I. Brümmer, K. N. Timmis and I. Wagner-Döbler, Metal selectivity of in situ microcolonies in biofilms of the Elbe River, *J. Bacteriol.*, 1997, **179**, 31-40.
23. S. Houot and J. Berthelin, Submicroscopic studies of iron deposits occurring in field drains - formation and evolution, *Geoderma*, 1992, **52**, 209-222.
24. D. Emerson and C. L. Moyer, Neutrophilic Fe-oxidizing bacteria are abundant at the Loihi Seamount hydrothermal vents and play a major role in Fe oxide deposition, *Appl. Environ. Microbiol.*, 2002, **68**, 3085-3093.
25. S. C. Neubauer, D. Emerson and J. P. Megonigal, Life at the energetic edge: Kinetics of circumneutral iron oxidation by lithotrophic iron-oxidizing bacteria isolated from the wetland-plant rhizosphere, *Appl. Environ. Microbiol.*, 2002, **68**, 3988-3995.
26. J. V. Weiss, D. Emerson and J. P. Megonigal, Rhizosphere iron(III) deposition and reduction in a *Juncus effusus* L.-dominated wetland, *Soil Sci. Soc. Am. J.*, 2005, **69**, 1861-1870.
27. T. Kasama and T. Murakami, The effects of microorganisms on Fe precipitation rates at netural pH, *Chem. Geol.*, 2001, **180**, 117-128.
28. D. Emerson and C. Moyer, Isolation and characterization of novel iron-oxidizing bacteria that grow at circumneutral pH, *App. Environ. Microbiol.*, 1997, **63**, 4784-4792.
29. L. Tuhela, L. Carlson and O. H. Tuovinen, Biogeochemical transformations of Fe and Mn in oxic groundwater and well water environments, *Environ. Sci. Heal. A* 1997, **32**, 407-426.
30. D. Emerson and N. P. Revsbech, Investigation of an iron-oxidizing microbial mat community located near Aarhus, Denmark- Laboratory studies, *Appl. Environ. Microbiol.*, 1994, **60**, 4032-4038.
31. E. D. Swanner, R. M. Nell and A. S. Templeton, *Ralstonia* species mediate Fe-oxidation in the deep biosphere of Henderson Mine, *Geochim. Cosmochim. Acta*, 2011, **74**, A1013-A1013.
32. C. S. Chan, G. De Stasio, S. A. Welch, M. Girasole, B. H. Frazer, M. V. Nesterova, S. Fakra and J. F. Banfield, Microbial polysaccharides template assembly of nanocrystal fibers, *Science*, 2004, **303**, 1656-1658.
33. T. D. Sowers, J. M. Harrington, M. L. Polizzotto and O. W. Duckworth, Sorption of arsenic to biogenic iron (oxyhydr) oxides produced in circumneutral environments, *Geochimica et Cosmochimica Acta*, 2017, **198**, 194-207.
34. R. M. Cornell and U. Schwertmann, *The iron oxides: structure, properties, reactions, occurrences and uses*, John Wiley & Sons, 2003.
35. J. A. Dyer, P. Trivedi, S. J. Sanders, N. C. Scrivner and D. L. Sparks, Treatment of zinc-contaminated water using a multistage ferrihydrite sorption system, *Journal of colloid and interface science*, 2004, **270**, 66-76.

36. P. Trivedi, J. A. Dyer and D. L. Sparks, Lead sorption onto ferrihydrite. 1. A macroscopic and spectroscopic assessment, *Environmental science & technology*, 2003, **37**, 908-914.
37. I. A. Katsoyiannis, H. Werner Althoff, H. Bartel and M. Jekel, The effect of groundwater composition on uranium(VI) sorption onto bacteriogenic iron oxides, *Water Research*, 2006, **40**, 3646-3652.
38. S. Langley, A. G. Gault, A. Ibrahim, Y. Takahashi, R. Renaud, D. Fortin, I. D. Clark and F. G. Ferris, Sorption of strontium onto bacteriogenic iron oxides, *Environmental science & technology*, 2009, **43**, 1008-1014.
39. A. L. Bussan and T. J. Strathmann, Influence of organic ligands on the reduction of polyhalogenated alkanes by iron (II), *Environmental science & technology*, 2007, **41**, 6740-6747.
40. E. E. Roden, J. M. McBeth, M. Blöthe, E. M. Percak-Dennett, E. J. Fleming, R. R. Holyoke, G. W. Luther III, D. Emerson and J. Schieber, The microbial ferrous wheel in a neutral pH groundwater seep, *Frontiers in Microbiology*, 2012, **3**.
41. C. S. Chan, S. C. Fakra, D. C. Edwards, D. Emerson and J. F. Banfield, Iron oxyhydroxide mineralization on microbial extracellular polysaccharides, *Geochim. Cosmochim. Acta*, 2009, **73**, 3807-3818.
42. C. S. Chan, S. C. Fakra, D. Emerson, E. J. Fleming and K. J. Edwards, Lithotrophic iron-oxidizing bacteria produce organic stalks to control mineral growth: implications for biosignature formation, *Isme Journal*, 2011, **5**, 717-727.
43. J. B. Fein, C. J. Daughney, N. Yee and T. A. Davis, A chemical equilibrium model for metal adsorption onto bacterial surfaces, *Geochimica et Cosmochimica Acta*, 1997, **61**, 3319-3328.
44. A. G. Gault, A. Ibrahim, S. Langley, R. Renaud, Y. Takahashi, C. Boothman, J. R. Lloyd, I. D. Clark, F. G. Ferris and D. Fortin, Microbial and geochemical features suggest iron redox cycling within bacteriogenic iron oxide-rich sediments, *Chemical Geology*, 2011, **281**, 41-51.
45. K. Laufer, M. Nordhoff, H. Røy, C. Schmidt, S. Behrens, B. B. Jørgensen and A. Kappler, Coexistence of microaerophilic, nitrate-reducing, and phototrophic Fe (II) oxidizers and Fe (III) reducers in coastal marine sediment, *Applied and environmental microbiology*, 2016, **82**, 1433-1447.
46. J. A. Rentz, I. P. Turner and J. L. Ullman, Removal of phosphorus from solution using biogenic iron oxides, *Water research*, 2009, **43**, 2029-2035.
47. I. A. Katsoyiannis, Carbonate effects and pH-dependence of uranium sorption onto bacteriogenic iron oxides: kinetic and equilibrium studies, *Journal of hazardous materials*, 2007, **139**, 31-37.
48. R. E. Martinez, K. Pedersen and F. G. Ferris, Cadmium complexation by bacteriogenic iron oxides from a subterranean environment, *Journal of colloid and interface science*, 2004, **275**, 82-89.
49. Y. M. Nelson, L. W. Lion, M. L. Shuler and W. C. Ghiorse, Effect of oxide formation mechanisms on lead adsorption by biogenic manganese (hydr) oxides, iron (hydr) oxides, and their mixtures, *Environmental science & technology*, 2002, **36**, 421-425.
50. E. M. Moon and C. L. Peacock, Adsorption of Cu (II) to ferrihydrite and ferrihydrite–bacteria composites: importance of the carboxyl group for Cu mobility in natural environments, *Geochimica et Cosmochimica Acta*, 2012, **92**, 203-219.

51. H. I. Adegoke, F. A. Adekola, O. S. Fatoki and B. J. Ximba, Sorptive Interaction of Oxyanions with Iron Oxides: A Review, *Polish Journal of Environmental Studies*, 2013, **22**.
52. S. Fendorf, M. J. Eick, P. Grossl and D. L. Sparks, Arsenate and Chromate Retention Mechanisms on Goethite. 1. Surface Structure, *Environmental Science & Technology*, 1997, **31**, 315-320.
53. X.-Z. Yu and X.-H. Zhang, Kinetics for adsorptive removal of chromium (VI) from aqueous solutions by ferri hydroxide/oxohydroxides, *Ecotoxicology*, 2014, **23**, 734-741.
54. J. M. Zachara, D. C. Girvin, R. L. Schmidt and C. T. Resch, Chromate adsorption on amorphous iron oxyhydroxide in the presence of major groundwater ions, *Environmental Science & Technology*, 1987, **21**, 589-594.
55. F. Ferris, K. Konhauser, B. Lyven and K. Pedersen, Accumulation of metals by bacteriogenic iron oxides in a subterranean environment, *Geomicrobiology Journal*, 1999, **16**, 181-192.
56. N. Almaraz, A. H. Whitaker, M. Y. Andrews and O. W. Duckworth, Assessing Biomineral Formation by Iron□oxidizing Bacteria in a Circumneutral Creek, *Journal of Contemporary Water Research & Education*, 2017, **160**, 60-71.
57. M. Y. Andrews and O. Duckworth, A universal assay for the detection of siderophore activity in natural waters, *Biometals*, 2016, **29**, 1085-1095.
58. U. Schwertmann and R. M. Cornell, *Iron oxides in the laboratory: preparation and characterization*, John Wiley & Sons, 2008.
59. L. L. Stookey, Ferrozine---a new spectrophotometric reagent for iron, *Anal. Chem.*, 1970, **42**, 779-781.
60. C. R. Gibbs, Characterization and application of FerroZine iron reagent as a ferrous iron indicator, *Anal. Chem.*, 1976, **48**, 1197-1201.
61. E. Fischer, B. Strehlow, D. Hartz and V. Braun, Soluble and membrane-bound ferrisiderophore reductases of Escherichia coli K-12, *Archives of microbiology*, 1990, **153**, 329-336.
62. J. P. Adjimani and E. Owusu, Nonenzymatic NADH/FMN-dependent reduction of ferric siderophores, *Journal of inorganic biochemistry*, 1997, **66**, 247-252.
63. H. Dailey and J. Lascelles, Reduction of iron and synthesis of protoheme by Spirillum itersonii and other organisms, *Journal of bacteriology*, 1977, **129**, 815-820.
64. D. Naka, D. Kim and T. J. Strathmann, Abiotic reduction of nitroaromatic compounds by aqueous iron (II)− catechol complexes, *Environmental science & technology*, 2006, **40**, 3006-3012.
65. D. Kim and T. J. Strathmann, Role of organically complexed iron (II) species in the reductive transformation of RDX in anoxic environments, *Environmental science & technology*, 2007, **41**, 1257-1264.
66. D. Naka, D. Kim, R. F. Carbonaro and T. J. Strathmann, Abiotic reduction of nitroaromatic contaminants by iron (II) complexes with organothiol ligands, *Environmental toxicology and chemistry*, 2008, **27**, 1257-1266.
67. D. E. Canfield, B. Thamdrup and J. W. Hansen, The anaerobic degradation of organic matter in Danish coastal sediments: iron reduction, manganese reduction, and sulfate reduction, *Geochimica et Cosmochimica Acta*, 1993, **57**, 3867-3883.

68. J. D. Kubicki, N. Kabengi, M. Chrysochoou and N. Bompoti, Density functional theory modeling of chromate adsorption onto ferrihydrite nanoparticles, *Geochemical Transactions*, 2018, **19**, 8.
69. B. R. James and R. J. Bartlett, Behavior of chromium in soils: VII. Adsorption and reduction of hexavalent forms, *Journal of Environmental Quality*, 1983, **12**, 177-181.
70. T. H. Hsia, S. L. Lo, C. F. Lin and D. Y. Lee, Chemical and spectroscopic evidence for specific adsorption of chromate on hydrous iron oxide, *Chemosphere*, 1993, **26**, 1897-1904.
71. E. Álvarez-Ayuso, A. García-Sánchez and X. Querol, Adsorption of Cr(VI) from synthetic solutions and electroplating wastewaters on amorphous aluminium oxide, *Journal of Hazardous Materials*, 2007, **142**, 191-198.
72. R. Bartlett and B. James, 1996.
73. Y. Wang, J. Ma and K. Chen, Adsorptive removal of Cr(vi) from wastewater by [small alpha]-FeOOH hierarchical structure: kinetics, equilibrium and thermodynamics, *Physical Chemistry Chemical Physics*, 2013, **15**, 19415-19421.
74. C. P. Johnston and M. Chrysochoou, Mechanisms of chromate adsorption on hematite, *Geochimica et Cosmochimica Acta*, 2014, **138**, 146-157.
75. O. Ajouyed, C. Hurel, M. Ammari, L. B. Allal and N. Marmier, Sorption of Cr(VI) onto natural iron and aluminum (oxy)hydroxides: Effects of pH, ionic strength and initial concentration, *Journal of Hazardous Materials*, 2010, **174**, 616-622.
76. C. H. Bolster and G. M. Hornberger, On the use of linearized Langmuir equations, *Soil Science Society of America Journal*, 2007, **71**, 1796-1806.
77. S. Kelly, D. Hesterberg and B. Ravel, Analysis of soils and minerals using X-ray absorption spectroscopy, *Methods of soil analysis. Part*, 2008, **5**, 387-463.
78. S. Webb, SIXpack: a graphical user interface for XAS analysis using IFEFFIT, *Physica scripta*, 2005, **2005**, 1011.
79. M. Newville, IFEFFIT: interactive XAFS analysis and FEFF fitting, *Journal of synchrotron radiation*, 2001, **8**, 322-324.
80. N. A. Rivera, D. Hesterberg, N. Kaur and O. W. Duckworth, Chemical Speciation of Potentially Toxic Trace Metals in Coal Fly Ash Associated with the Kingston Fly Ash Spill, *Energy & Fuels*, 2017, **31**, 9652–9659.
81. J. M. Harrington, J. R. Bargar, A. A. Jarzecki, J. G. Roberts, L. A. Sombers and O. W. Duckworth, Trace metal complexation by the triscatecholate siderophore protochelin: structure and stability, *BioMetals*, 2012, **25**, 393-412.
82. J. M. Harrington, D. L. Parker, J. R. Bargar, A. A. Jarzecki, B. M. Tebo, G. Sposito and O. W. Duckworth, Structural dependence of Mn complexation by siderophores: donor group dependence on complex stability and reactivity, *Geochimica et Cosmochimica Acta*, 2012, **88**, 106-119.
83. P. A. O'day, N. Rivera, R. Root and S. A. Carroll, X-ray absorption spectroscopic study of Fe reference compounds for the analysis of natural sediments, *American Mineralogist*, 2004, **89**, 572-585.
84. O. W. Duckworth, M. M. Akafia, M. Y. Andrews and J. R. Bargar, Siderophore-promoted dissolution of chromium from hydroxide minerals, *Environmental Science: Processes & Impacts*, 2014, **16**, 1348 - 1359.

85. E. M. Saad, J. Sun, S. Chen, O. J. Borkiewicz, M. Zhu, O. W. Duckworth and Y. Tang, Siderophore and Organic Acid Promoted Dissolution and Transformation of Cr(III)-Fe(III)-(oxy)hydroxides, *Environ. Sci. Technol.*, 2017, **51**, 3223-3232.
86. M.-P. Isaure, A. Laboudigue, A. Manceau, G. Sarret, C. Tiffreau, P. Trocellier, G. Lamble, J.-L. Hazemann and D. Chateigner, Quantitative Zn speciation in a contaminated dredged sediment by μ-PIXE, μ-SXRF, EXAFS spectroscopy and principal component analysis, *Geochimica et Cosmochimica Acta*, 2002, **66**, 1549-1567.
87. A. Manceau, B. Lanson, M. L. Schlegel, J. C. Harge, M. Musso, L. Eybert-Berard, J.-L. Hazemann, D. Chateigner and G. M. Lamble, Quantitative Zn speciation in smelter-contaminated soils by EXAFS spectroscopy, *American Journal of Science*, 2000, **300**, 289-343.
88. A. C. Cismasu, F. M. Michel, A. P. Tcaciuc, T. Tyliszczak and G. E. Brown Jr, Composition and structural aspects of naturally occurring ferrihydrite, *Comptes Rendus Geoscience*, 2011, **343**, 210-218.
89. C. B. Kennedy, S. D. Scott and F. G. Ferris, Characterization of bacteriogenic iron oxide deposits from Axial Volcano, Juan de Fuca Ridge, northeast Pacific Ocean, *Geomicrobiology journal*, 2003, **20**, 199-214.
90. D. R. Lovley and E. J. Phillips, Organic matter mineralization with reduction of ferric iron in anaerobic sediments, *Applied and environmental microbiology*, 1986, **51**, 683-689.
91. F. M. Michel, V. Barrón, J. Torrent, M. P. Morales, C. J. Serna, J.-F. Boily, Q. Liu, A. Ambrosini, A. C. Cismasu and G. E. Brown, Ordered ferrimagnetic form of ferrihydrite reveals links among structure, composition, and magnetism, *Proceedings of the National Academy of Sciences*, 2010, **107**, 2787-2792.
92. D. Adhikari, Q. Zhao, K. Das, J. Mejia, R. Huang, X. Wang, S. R. Poulson, Y. Tang, E. E. Roden and Y. Yang, Dynamics of ferrihydrite-bound organic carbon during microbial Fe reduction, *Geochimica et Cosmochimica Acta*, 2017, **212**, 221-233.
93. A. C. Cismasu, F. M. Michel, J. F. Stebbins, C. Levard and G. E. Brown, Properties of impurity-bearing ferrihydrite I. Effects of Al content and precipitation rate on the structure of 2-line ferrihydrite, *Geochimica et Cosmochimica Acta*, 2012, **92**, 275-291.
94. A. C. Cismasu, F. M. Michel, A. P. Tcaciuc and G. E. Brown, Properties of impurity-bearing ferrihydrite III. Effects of Si on the structure of 2-line ferrihydrite, *Geochimica et Cosmochimica Acta*, 2014, **133**, 168-185.
95. A. H. M. Whitaker, F. Marc, Peak D.; Thompson, A.; Duckworth, Owen W, presented in part at the American Chemical Society, San Francisco, CA, 2017.
96. C. M. van Genuchten, A. J. Gadgil and J. Peña, Fe(III) Nucleation in the Presence of Bivalent Cations and Oxyanions Leads to Subnanoscale 7 Å Polymers, *Environmental Science & Technology*, 2014, **48**, 11828-11836.
97. B. M. Toner, C. M. Santelli, M. A. Marcus, R. Wirth, C. S. Chan, T. McCollom, W. Bach and K. J. Edwards, Biogenic iron oxyhydroxide formation at mid-ocean ridge hydrothermal vents: Juan de Fuca Ridge, *Geochim. Cosmochim. Acta*, 2009, **73**, 388-403.
98. B. M. Toner, T. S. Berquó, F. M. Michel, J. V. Sorensen, A. S. Templeton and K. J. Edwards, Mineralogy of iron microbial mats from Loihi Seamount, *Frontiers in microbiology*, 2012, **3**.

99. C. Childs, C. Downes and N. Wells, Hydrous iron oxide minerals with short range order deposited in a spring/stream system, Tongariro National Park, New Zealand, *Soil Research*, 1982, **20**, 119-129.
100. G. Sposito, *The surface chemistry of soils*, Oxford University Press, 1984.
101. Y. Wang, A. Gélabert, F. M. Michel, Y. Choi, J. Gescher, G. Ona-Nguema, P. J. Eng, J. R. Bargar, F. Farges and A. M. Spormann, Effect of biofilm coatings at metal-oxide/water interfaces I: Pb (II) and Zn (II) partitioning and speciation at Shewanella oneidensis/metal-oxide/water interfaces, *Geochimica et Cosmochimica Acta*, 2016, **188**, 368-392.
102. G. K. Druschel, D. Emerson, R. Sutka, P. Suchecki and G. W. Luther, Low-oxygen and chemical kinetic constraints on the geochemical niche of neutrophilic iron (II) oxidizing microorganisms, *Geochimica et Cosmochimica Acta*, 2008, **72**, 3358-3370.
103. P. C. Singer and W. Stumm, Acidic Mine Drainage: The Rate-Determining Step, *Science*, 1970, **167**, 1121-1123.
104. K. A. Weber, L. A. Achenbach and J. D. Coates, Microorganisms pumping iron: anaerobic microbial iron oxidation and reduction, *Nature Reviews Microbiology*, 2006, **4**, 752-764.
105. S. T. Martin, in *Environmental Catalysis*, ed. V. H. Grassian, Marcel-Dekker, CRC Press, Boca Raton, 2005, pp. 61-81.
106. V. I. Rich and R. M. Maier, in *Environmental Microbiology (Third Edition)*, Elsevier, 2015, pp. 111-138.
107. E. C. W. Rieb, Andrew H; Duckworth, Owen W, presented in part at the Soil Science Society of America, Tampa, Fl, 2017.
108. I. J. Buerge and S. J. Hug, Kinetics and pH dependence of chromium (VI) reduction by iron (II), *Environmental science & technology*, 1997, **31**, 1426-1432.
109. R. J. Kieber, S. A. Skrabal, B. J. Smith and J. D. Willey, Organic Complexation of Fe(II) and Its Impact on the Redox Cycling of Iron in Rain, *Environmental Science & Technology*, 2005, **39**, 1576-1583.
110. R. P. Schwarzenbach, W. Angst, C. Holliger, S. J. Hug and J. Klausen, Reductive transformations of anthropogenic chemicals in natural and technical systems, *CHIMIA International Journal for Chemistry*, 1997, **51**, 908-914.
111. L. Eary and D. Rai, Chromate reduction by subsurface soils under acidic conditions, *Soil Science Society of America Journal*, 1991, **55**, 676-683.
112. W. A. Clarke, K. O. Konhauser, J. C. Thomas and S. H. Bottrell, Ferric hydroxide and ferric hydroxysulfate precipitation by bacteria in an acid mine drainage lagoon, *FEMS Microbiology Reviews*, 1997, **20**, 351-361.
113. S. C. Haaijer, H. R. Harhangi, B. B. Meijerink, M. Strous, A. Pol, A. J. Smolders, K. Verwegen, M. S. Jetten and H. J. O. Den Camp, Bacteria associated with iron seeps in a sulfur-rich, neutral pH, freshwater ecosystem, *The ISME journal*, 2008, **2**, 1231.
114. A. Thompson, C. Chen, N. Noor, C. A. Hodges, D. Barcellos and D. Richter, New Orleans, Louisiana, 2017.

**Figure Captions**

**Figure 1.** Fe K-edge EXAFS spectra for pre-Cr sorption (Day 0) and post-Cr sorption (Day 14) 2LFh, BIOS, and BIOS with 0.135 M ferrozine plotted with Fe(III) mineral standard spectra. LCFs are shown as black dotted-lines, with fit parameters in **Table 1**). Initial experimental conditions: 1 g $L^{-1}$ sorbent (dry weight basis), Cr(VI) = 0.96 mM, I = 0.01 M NaCl, pH = 7.0 ± 0.2.

**Figure 2.** (A) BET SSA normalized sorption of Cr onto 2LFh (red circles), BIOS (orange triangles), and BIOS with 0.135 M ferrozine (purple squares) as a function of time and (B) total dissolved Fe concentrations for 2LFh (red circles), BIOS (orange triangles), and BIOS with 0.135 M ferrozine (purple squares) as a function of time. Production of dissolved Fe(II) as a function of time (open symbols) is also shown for the BIOS with 0.135 M ferrozine treatment. Initial experimental conditions: 1 g $L^{-1}$ sorbent (dry weight basis), Cr(VI) = 0.96 mM, I = 0.01 M NaCl, pH = 7.0 ± 0.2.

**Figure 3.** BET SSA normalized sorption of Cr onto 2LFh (red circles) and BIOS (orange triangles) as a function of dissolved Cr. All sorption data was modeled with a Freundlich fit. Data points from day 3 of sorption rate experiments (**Figure 2**) are also shown for 2LFh and BIOS (open symbols). Initial experimental conditions: 1 g $L^{-1}$ sorbent (dry weight basis), Cr(VI) = 0–1.92 mM, I = 0.01 M NaCl, pH = 7.0 ± 0.2. The Freundlich sorption constant ($K_f$) and exponential constant ($n$) for 2LFh was 0.009 ± 0.005 μmol Cr $m^{-2}$ and 0.69 ± 0.07, respectively, whereas, for BIOS they were 0.020 ± 0.006 μmol Cr $m^{-2}$ and 0.63 ± 0.04, respectively. Uncertainty in isotherm parameters is reported as standard error.

**Figure 4.** Cr K-edge XANES spectra for (A) 2LFh, (B) BIOS, and (C) BIOS with 0.135 M ferrozine at day 1, 3, 7, and 14 plotted with Cr oxidation state standard spectra (100% $Cr_2O_3$ (100% Cr(III)), 50% $Cr_2O_3$/50% $K_2CrO_4$, and 100% $K_2CrO_4$ (100 mol% Cr(VI))). (D) A linear regression relating the integrated intensity of the Cr(VI) pre-edge peak at 5993.3 eV to the oxidation state of the Cr standards. (E) The mole% Cr(VI) in 2LFh, BIOS, and BIOS with 0.135 M ferrozine as function of time. Initial experimental conditions: 1 g $L^{-1}$ sorbent (dry weight basis), Cr(VI) = 0.96 mM, I = 0.01 M NaCl, pH = 7.0 ± 0.2.

**Figure 5.** Cr K-edge XANES spectra for (A) BIOS plotted with Cr speciation standards (Cr(III)-rhizoferrin,[84] a Cr(III)-carboxylate complex; Cr2Fe8,[85] a Cr(III)-Fe(III)$(OH)_3$ species; and Cr(VI) sorbed to 2LFh, the 14 d sample from this study. LCFs are shown as dotted lines; (B) results of LCFs plotted as percentage of each component as a function of time. Initial experimental conditions: 1 g $L^{-1}$ sorbent (dry weight basis), Cr(VI) = 0.96 mM, I = 0.01 M NaCl, pH = 7.0 ± 0.2.

**Figure 6.** Amount of Cr(III) produced in BIOS experiments plotted against amount of Fe(II) generated in BIOS experiments with ferrozine at corresponding time points. Cr(III) data is derived from LCF fits (**Figure 5**) and Fe(II) data is from **Figure 2B**. Initial experimental conditions: 1 g $L^{-1}$ sorbent (dry weight basis), Cr(VI) = 0.96 mM, I = 0.01 M NaCl, pH = 7.0 ± 0.2.

**Figure 7.** Schematic depicting the proposed mechanism of Cr(VI) reduction by BIOS. The reaction is initiated by a one electron transfer from Fe(II) to Cr(VI), as shown by reaction 2 in the figure and text. The Cr(V) may then self-reduce (reaction 3 in the figure and text) or react

with organic matter to produce Cr(III) complexes (reaction 4 in the figure and text). At longer times, Cr(III) is sequestered by the mineral phase (reaction 5 in the figure).

**Table 1.** Fe EXAFS linear combination fits (LCFs) for pre-Cr sorption (Day 0) and post-Cr sorption (Day 14) 2LFh and BIOS. LCFs were performed in SIXPACK and normalized to 100%, with raw fits summing 100 ± 30%. Error is reported from the software output but is estimated to be 10%.

| Sample ID | Component | % Contribution | R-value |
|---|---|---|---|
| 2LFh D0 | Ferrihydrite | 100 ± 2 | 0.058 |
| BIOS D0 | Ferrihydrite | 80 ± 4 | 0.024 |
| | HFO with Si | 20 ± 2 | |
| 2LFh D14 | Ferrihydrite | 100 ± 2 | 0.053 |
| BIOS D14 | Ferrihydrite | 74 ± 4 | 0.026 |
| | HFO with Si | 26 ± 3 | |
| BIOS with ferrozine D14 | Ferrihydrite | 74 ± 3 | 0.019 |
| | HFO with Si | 26 ± 2 | |

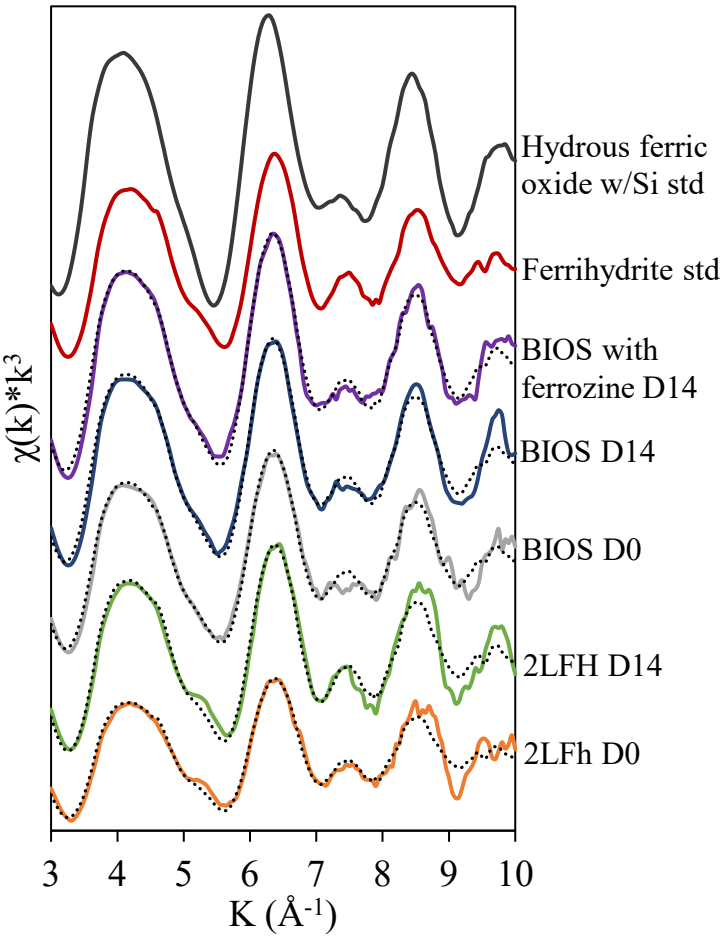
Hydrous ferric oxide w/Si std
Ferrihydrite std
BIOS with ferrozine D14
BIOS D14
BIOS D0
2LFH D14
2LFh D0
χ(k)*k3
3 4 5 6 7 8 9 10
K (Å-1)

**Figure 1.**

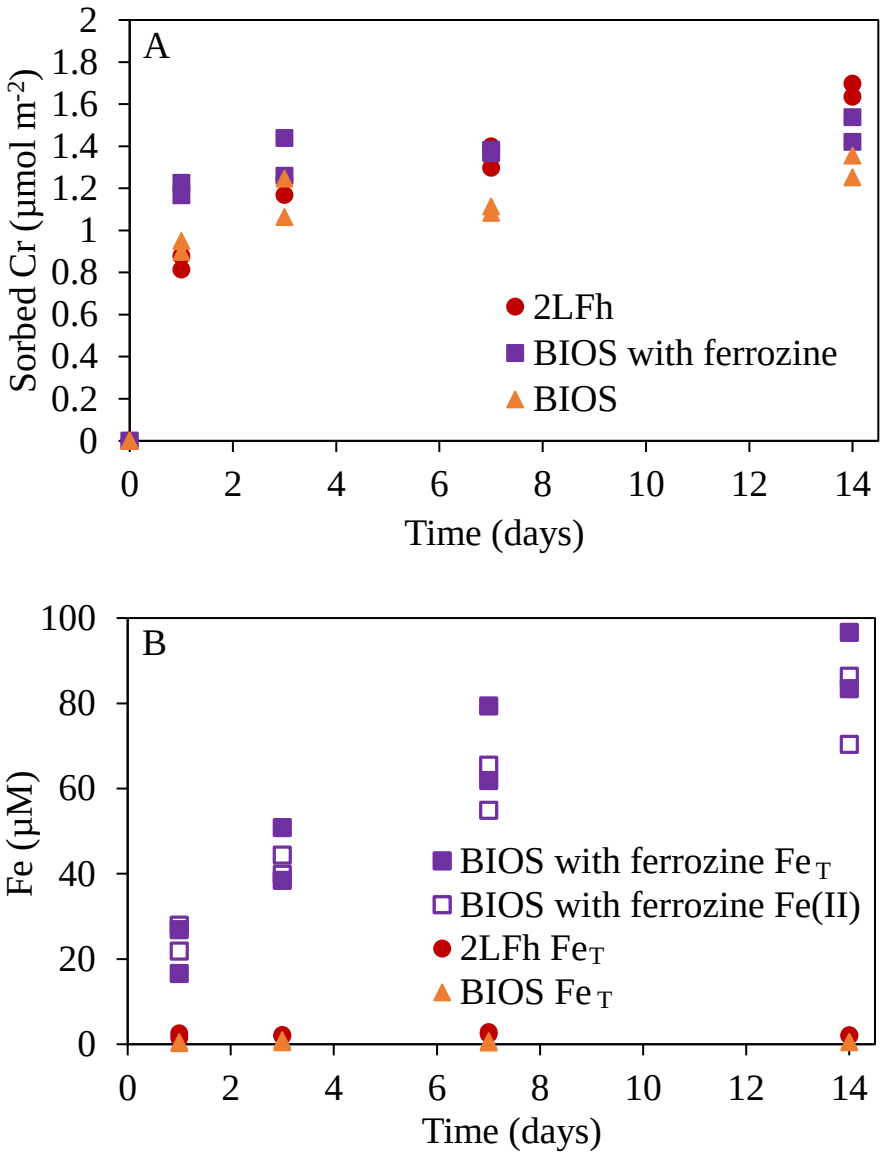
A
Sorbed Cr (µmol m-2)
2
1.8
1.6
1.4
1.2
1
0.8
0.6
0.4
0.2
0
0
2
4
6
8
10
12
14
Time (days)
2LFh
BIOS with ferrozine
BIOS
B
Fe (µM)
100
80
60
40
20
0
0
2
4
6
8
10
12
14
Time (days)
BIOS with ferrozine FeT
BIOS with ferrozine Fe(II)
2LFh FeT
BIOS FeT

**Figure 2.**

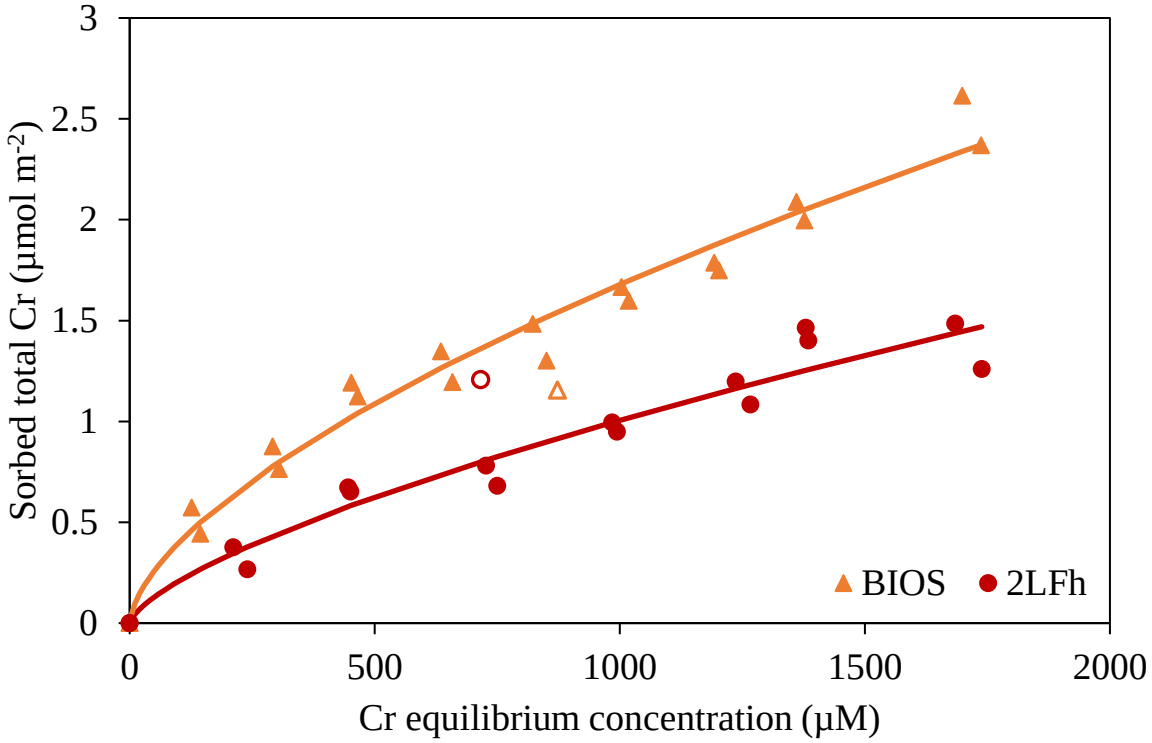
3
2.5
2
1.5
1
0.5
0
Sorbed total Cr (µmol m-2)
0
500
1000
1500
2000
Cr equilibrium concentration (µM)
BIOS
2LFh

**Figure 3.**

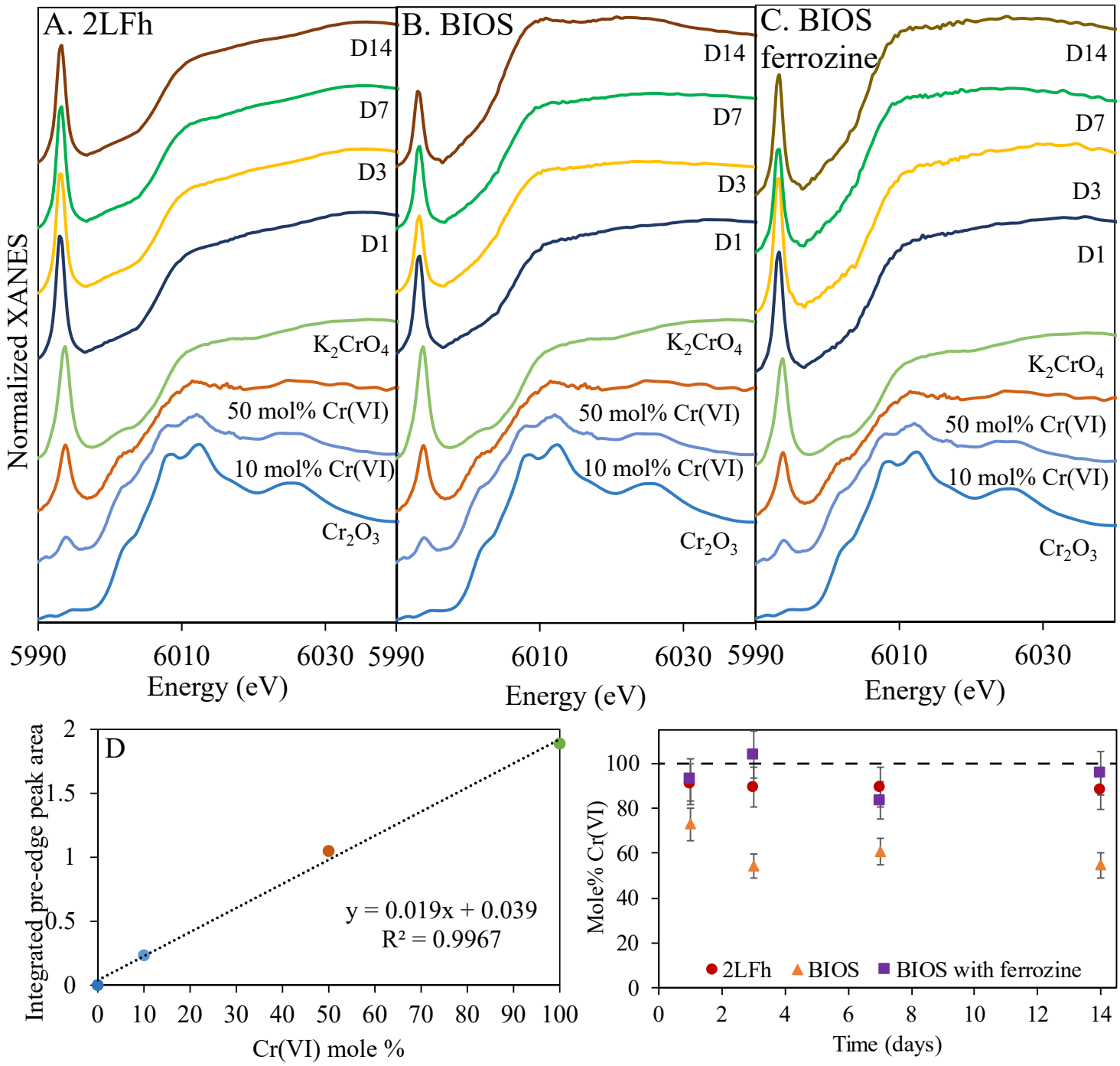
A. 2LFh
B. BIOS
C. BIOS ferrozine
D14
D7
D3
D1
K2CrO4
50 mol% Cr(VI)
10 mol% Cr(VI)
Cr2O3
Normalized XANES
5990
6010
6030
Energy (eV)
D
Integrated pre-edge peak area
Cr(VI) mole %
y = 0.019x + 0.039
R² = 0.9967
Mole% Cr(VI)
Time (days)
2LFh
BIOS
BIOS with ferrozine

**Figure 4.**

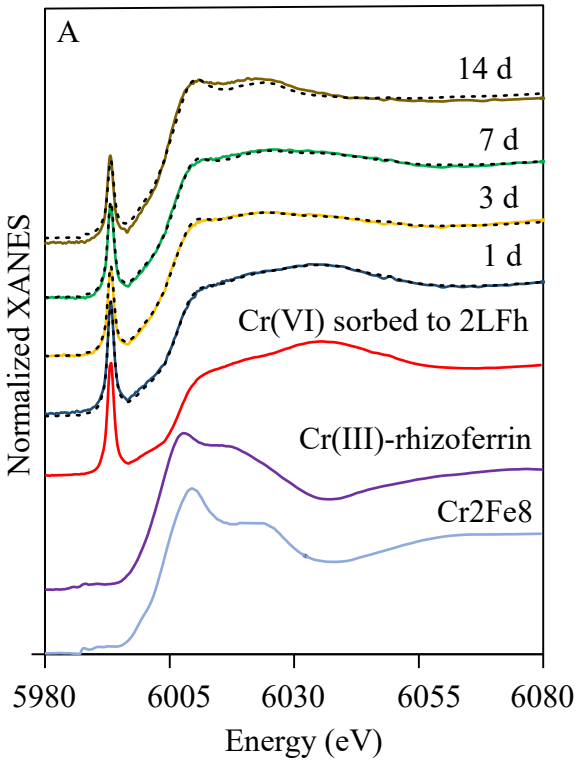
A
14 d
7 d
3 d
1 d
Cr(VI) sorbed to 2LFh
Cr(III)-rhizoferrin
Cr2Fe8
Normalized XANES
5980
6005
6030
6055
6080
Energy (eV)

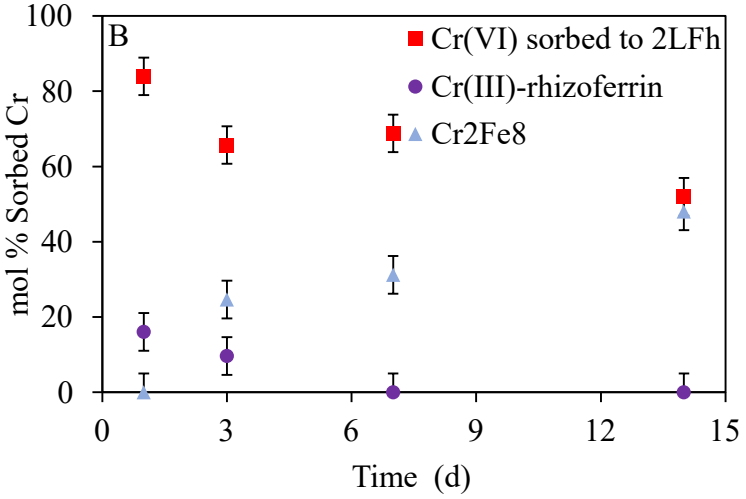
B
Cr(VI) sorbed to 2LFh
Cr(III)-rhizoferrin
Cr2Fe8
mol % Sorbed Cr
0
20
40
60
80
100
0
3
6
9
12
15
Time (d)

**Figure 5.**

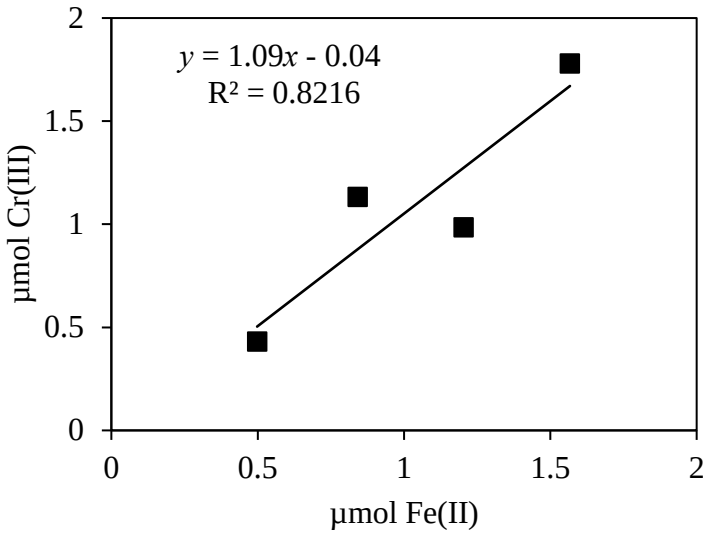


**Figure 6.**

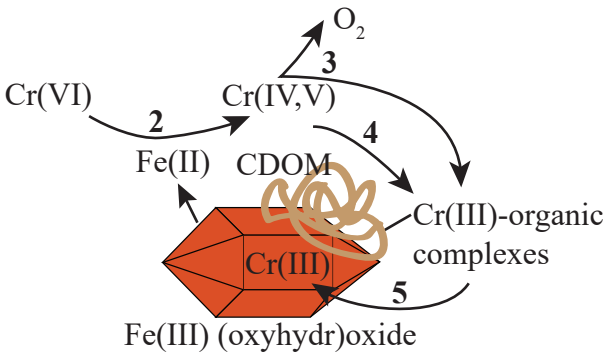
O2
3
Cr(VI)
2
Cr(IV,V)
4
Fe(II)
CDOM
Cr(III)-organic
complexes
Cr(III)
5
Fe(III) (oxyhydr)oxide

Figure 7.

**Table of Contents Entry.**

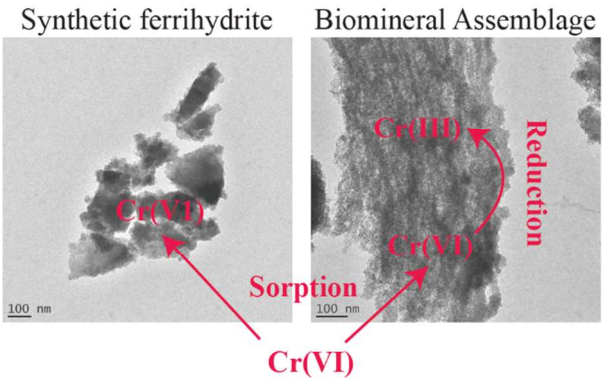


Biogenic iron (oxyhydr)oxides adsorb dissolved Cr(VI), as well as promote its reduction to less mobile and toxic Cr(III) via a Fe(II) mediated process.